E. V. Gryzlova, A. I. Magunov, I. Rotter,
S. I. Strakhova.

Laser polarization control of autoionization in helium atom.

Preprint of NPI MSU 2005-12/778

LOMONOSOV MOSCOW STATE UNIVERSITY

SKOBELTSYN INSTITUTE OF NUCLEAR PHYSICS.

E. V. Gryzlova, A. I. Magunov, I. Rotter,
S. I. Strakhova.

Laser polarization control of autoionization in helium atom.

Preprint of NPI MSU 2005-12/778

УДК 537.563.5:621.375.8

Gryzlova E. V., Magunov A. I., Rotter I., Strakhova S. I.

Laser polarization control of autoionization in helium atom.

str@sinp.msu.ru

Preprint of NPI MSU 2005-12/778

The resonance coupling of the $2s2p\,^1P$ and $2s3d\,^1D$ autoionizing states in the helium atom by a laser field with arbitrary polarization is studied in the framework of the non-Hermitian effective Hamiltonian approach. We provide the analytical expression for the photoionization cross section of the ground state by the VUV probe radiation with arbitrary polarization in the vicinity of the $2s2p\,^1P$ state. The calculations demonstrate strong changes in the resonance structure of the cross section with variation of the probe and laser polarizations. The effect is caused by the interference of different transitions between the laser-coupled manifold of magnetic sublevels.

Грызлова Е. В., Магунов А. И., Роттер И., Страхова С. И.

Автоионизация атома гелия в присутствии лазерных полей разной поляризации.

Препринт НИИЯФ МГУ 2005-12/778

В рамках метода неэрмитового эффективного гамильтониана изучена резонансная связь произвольно поляризованным лазерным полем $2s2p\,^1P$ и $2s3d\,^1D$ автоионизационных состояний в атоме гелия. Получены аналитические выражения для сечения фотоионизации из основного состояния в окрестность $2s2p\,^1P$ состояния пробным ВУФ излучением, произвольным образом поляризованным. Расчеты демонстрируют сильное изменение резонансной структуры сечения фотоионизации при изменении поляризации лазерного и пробного полей. Эффект обусловлен интерференцией различных переходов между связанными лазером магнитными подуровнями.

Introduction

During resent years many interesting effects caused by the interference of different resonance transitions in quantum systems have been studied. Different resonance states are investigated experimentally and theoretically in atoms using the laser-induced transitions between excited and autoionizing states (see, for example, [1 - 12]. Usually, the problem is considered with linearly polarized pumping or dressing laser and probe radiations. Under this condition, the number of states involved in the resonance transitions is minimized. The resonance structures are studied as a function of laser intensity and frequency detuning from the transition energy.

The polarization has been shown in [13] to play an important role for the observed resonance structures. In this work, the laser induced continuum structure is observed in the cesium atom by using a combination of linearly and circularly polarized light. Later a similar effect was studied in other atoms [14, 15]. The polarization dependent quantum beats in the photoionization are studied in [16]. They result from interferences between the different transitions via the fine structure states. In rubidium, the polarization plays an important role for the electromagnetically induced transparency in cascade transitions between hyperfine sublevels as shown in [17 - 19]. Orientation and alignment of atoms and molecules by elliptically polarized light are analyzed in [20]. The observed effects are caused by the coupling between Zeeman sublevels which is analyzed in [21, 22] for discrete states in an elliptically polarized laser field. The creation of stationary coherent states in a system with laser coupled degenerate states is studied in [23] as well, and the most recent results are presented in [24]. Spin-polarized photoelectron production suggested many years ago by Fano [25], is studied recently for different combinations of the pump-probe polarization [26, 27]. Polarization sensitive three-photon autoionization is studied in [28, 29]. As a result, the laser polarization can essentially influence the interferences that are induced in the resonance coupling between the autoionizing states.

In this work we consider the coupling of the $2s2p\,^1P$ and $2s3d\,^1D$ autoionizing states in helium by elliptically polarized laser radiation. The coupling effects are examined in the photoabsorption cross section of the probe radiation with different polarization and propagation direction with respect to the laser wave vector. The so-called non-Hermitian effective Hamiltonian approach is used which

describes the behavior of different systems with overlapping resonant states [30, 31]. The scheme in Fig. 1 shows all resonant couplings between the magnetic sublevels of the AISs in He which are induced by the elliptically polarized laser field, as well as the transitions that are induced by the probe radiation from the ground state to the continuum in the vicinity of ^{1}P state.

Atomic units are used throughout the paper.

Theory

In the dipole approximation the interaction of an atom with the laser and probe radiation is defined by

$$\mathbf{H}_{\text{int}} = -\mathbf{D}\cdot\left[\mathbf{F}(t)+\mathbf{f}(t)\right]. \tag{1}$$

Here **D** is the dipole momentum of the atom. The local field strength of the laser radiation with angular frequency ω and wave vector $\mathbf{k}=\mathbf{n}_z\omega/c$ is

$$\begin{aligned}\mathbf{F}(t) &= F\left[\, a\cos(\omega t)\mathbf{n}_x + \sqrt{1-a^2}\,\cos(\omega t+\varphi)\mathbf{n}_y \,\right] = \\ &= \frac{F}{2}\left[(\alpha\mathbf{n}_1 + \beta\mathbf{n}_{-1})\exp(-i\omega t) + c.c.\right].\end{aligned} \tag{2}$$

in Cartesian and cyclic coordinates, correspondingly. The parameters a and φ define the ellipticity of the polarization $P = 2a\sqrt{1-a^2}\,\sin(\varphi)$ with the helicity defined by the sign of $\sin(\varphi)$. The cyclic unit vectors are defined by the relations $\mathbf{n}_{\pm1} = \mp\left(\mathbf{n}_x \pm i\mathbf{n}_y\right)/\sqrt{2}$, $\mathbf{n}_0 = \mathbf{n}_z$, and

$$\alpha = \frac{-a + i\sqrt{1-a^2}\,\exp(-i\varphi)}{\sqrt{2}},\quad \beta = \frac{a + i\sqrt{1-a^2}\,\exp(-i\varphi)}{\sqrt{2}}. \tag{3}$$

For $\varphi=\pi/2$ the ellipse is aligned along the x or y axis, and α and β are real values.

For the probe radiation propagating in the direction $\mathrm{n} = \mathrm{n}_y\sin(\theta) + \mathrm{n}_z\cos(\theta)$ with the angle θ relative to the direction **k**, we get

$$\begin{aligned}\mathbf{f}(t) &= f\left[\, b\cos(\Omega t)\mathbf{n}_x + \sqrt{1-b^2}\,\cos(\Omega t+\phi)\left(\cos(\Theta)\mathbf{n}_y + \sin(\Theta)\mathbf{n}_z\right)\right] = \\ &= \frac{f}{2}\left[\mathbf{e}\exp(-i\Omega t) + c.c.\right].\end{aligned} \tag{4}$$

with $\mathbf{e} = \varepsilon^{1}\mathbf{n}_1 + \varepsilon^{-1}\mathbf{n}_{-1} + \varepsilon^{0}\mathbf{n}_0$ and

$$\varepsilon^{1} = \frac{-b + i\cos(\theta)\sqrt{1-b^2}\,\exp(-i\phi)}{\sqrt{2}},$$
$$\varepsilon^{-1} = \frac{b + i\cos(\theta)\sqrt{1-b^2}\,\exp(-i\phi)}{\sqrt{2}} \qquad (5)$$
$$\varepsilon^{0} = -\sin(\theta)\sqrt{1-b^2}\,\exp(-i\phi).$$

where $\left|\varepsilon^{-1}\right|^2 + \left|\varepsilon^{1}\right|^2 + \left|\varepsilon^{0}\right|^2 = 1$.

In the rotating wave approximation, the couplings between the AISs (according to the scheme in Fig. 1) are described by the non-Hermitian effective Hamiltonian that contains two quasi diagonal cells,

$$\mathbf{H_{eff}} = \begin{bmatrix} \mathbf{H_0} & [0] \\ [0]^{+} & \mathbf{H_1} \end{bmatrix}. \qquad (6)$$

Each of the cells contains the laser-coupled magnetic sublevels (with the quantization axis along **k**) that correspond to the coupled resonances. By (6) they are uncoupled to those of the other cell. The fractional Hamiltonians are

$$\mathbf{H}_0 = \begin{bmatrix} \varepsilon_{D-1} & -\frac{1}{2}\Psi_{D-1,P0} & \frac{1}{2}\partial_{D-1,D1} \\ -\frac{1}{2}\Psi_{P0,D-1} & \varepsilon_{P0} & -\frac{1}{2}\Psi_{P0,D1} \\ \frac{1}{2}\partial_{D1,D-1} & -\frac{1}{2}\Psi_{D1,P0} & \varepsilon_{D1} \end{bmatrix} \qquad (7)$$

and

$$\mathbf{H}_1 = \begin{bmatrix} \varepsilon_{D-2} & -\frac{1}{2}\Psi_{D-2,P-1} & \frac{1}{2}\partial_{D-2,D0} & 0 & 0 \\ -\frac{1}{2}\Psi_{P-1,D-2} & \varepsilon_{P-1} & -\frac{1}{2}\Psi_{P-1,D0} & 0 & 0 \\ \frac{1}{2}\partial_{D0,D-2} & -\frac{1}{2}\Psi_{D0,P-1} & \varepsilon_{D0} & -\frac{1}{2}\Psi_{D0,P1} & \frac{1}{2}\partial_{D0,D2} \\ 0 & 0 & -\frac{1}{2}\Psi_{P1,D0} & \varepsilon_{P1} & -\frac{1}{2}\Psi_{P1,D2} \\ 0 & 0 & \frac{1}{2}\partial_{D2,D0} & -\frac{1}{2}\Psi_{D2,P1} & \varepsilon_{D2} \end{bmatrix} \qquad (8)$$

Here the diagonal matrix elements

$$\mathcal{E}_{PM} = E_P + \alpha_{PM} I - i\frac{\Gamma_P}{2}, \quad \mathcal{E}_{DM} = E_D - \omega + \alpha_{DM} - i\frac{\Gamma_D + \gamma_{DM}}{2}. \qquad (9)$$

are defined by the energies E_L and widths Γ_L of the autoionizing states, the laser-induced energy shifts (α_{LM} are the corresponding dynamical polarizabilities), and the ionization width of the ^{1}DM states due to the single electron transitions 2s3d→2sEp, 2sEf

$$\gamma_{\mathrm{DM}} = 2\pi I \sum_{L} \frac{\left|d_{E_{\mathrm{D}}+\omega L,\mathrm{D}}\right|^2}{2L+1}\left[|\alpha|^2\left(C^{LM+1}_{2M,11}\right)^2 + |\beta|^2\left(C^{LM-1}_{2M,1-1}\right)^2\right]. \quad (10)$$

at the intensity $I = \frac{1}{4}F^2$ (1 a.u.=1.4 · 10^{17} W/cm^2).

The $d_{El,D} = (2L+1)(EL0|d_0|D0)/C^{L0}_{20,10}$ are the reduced dipole matrix elements according to the Wigner-Eckart theorem, and the $C^{jm}_{j_1m_1,j_2m_2}$ are the Clebsch-Gordan coefficients.

The non-diagonal matrix elements for the direct P-D coupling are defined by the Rabi frequencies

$$\Omega_{\mathrm{DM',PM}} = \frac{d_{\mathrm{D,P}}F}{\sqrt{5}}\left(\alpha C^{2M'}_{1M,11} + \beta C^{2M'}_{1M,1-1}\right). \quad (11)$$

and those for the two-photon coupling via the continuum above the second threshold by

$$\gamma_{\mathrm{DM}} = 2\pi I\alpha\beta^*\left(Q_{M+2,M} - i\right)\sum_{L}\frac{\left|d_{E_{\mathrm{D}}+\omega L,\mathrm{D}}\right|^2}{2L+1}C^{LM+1}_{2M,11}C^{LM+1}_{2M+2,1-1}\,. \quad (12)$$

The $Q_{M',M}$ are defined by

$$Q_{M+2,M} = \frac{\alpha_{M+2,2} + P\int dE g(E)/(E_{\mathrm{D}} + u_l - E)}{pg(E_{\mathrm{D}} + u_l)}\,. \quad (13)$$

where the function $g(E_{\mathrm{D}} + u_l)$ is the sum in (12) and $\alpha_{M+2,M}$ is the non-diagonal analog of the dynamical polarizability. Usually, the value of $Q_{M',M}$ is small (cf. [12]).

The complex eigenvalues $\tilde{\mathcal{E}}_{LM}$ of (7) and (8) define the positions and widths of the overlapping resonances in the cross section [7,8]. Below we examine the photoabsorption cross section for the probe radiation that ionizes the atom from the ground state when exposed to the laser field (see Fig. 1).

Using the rotating wave approximation the photoionization cross section being laser-assisted by the probe radiation, is obtained as

$$\sigma(\Omega, F, \omega, \alpha, \varphi, b, \phi, \theta) = \sigma_a(\Omega)\left\{1 - \mathrm{Im}\left[\bar{\mathbf{t}}_0^T\left(\Omega\mathbf{1} - \mathbf{H}_0\right)^{-1}\mathbf{t}_0 + \bar{\mathbf{t}}_1^T\left(\Omega\mathbf{1} - \mathbf{H}_1\right)^{-1}\mathbf{t}_1\right]\right\}. \quad (14)$$

The vectors $\mathbf{t}_j$ and $\bar{\mathbf{t}}_j$ are defined by the transition amplitudes from the ground state

$$\bar{\mathbf{t}}_0^T = \left[\bar{t}_{\mathrm{D}-1}, \bar{t}_{\mathrm{P}0}, \bar{t}_{\mathrm{D}1}\right],\ \bar{\mathbf{t}}_1^T = \left[\bar{t}_{\mathrm{D}-2}, \bar{t}_{\mathrm{P}-1}, \bar{t}_{\mathrm{D}0}, \bar{t}_{\mathrm{P}1}, \bar{t}_{\mathrm{D}2}\right]. \quad (15)$$

with

$$t_{LM} = \sqrt{\frac{\Gamma_L}{2}}\rho_{LM}\left(q_L - i\right),\ \bar{t}_{LM} = \sqrt{\frac{\Gamma_L}{2}}\rho^*_{LM}\left(q_L - i\right). \tag{16}$$

where q_L and ρ_{LM} are the Fano parameters. In the case of one decay channel which is considered here, we have

$$\rho_{\mathrm{P}M} = \varepsilon^M \exp\left[i \arg\left(V_{\mathrm{P},E\mathrm{P}} d_{E\mathrm{P},0}\right)\right]. \tag{17}$$

$$\rho_{\mathrm{D}M'} = \frac{1}{\sqrt{5}}\left(\alpha C^{2M'}_{1M,11} + \beta C^{2M'}_{1M,1-1}\right)\sqrt{\frac{2\pi\left|d_{\mathrm{D},E\mathrm{P}}\right|^2 I}{\Gamma_{\mathrm{D}}}}\varepsilon^M \exp\left[i \arg\left(V_{\mathrm{D},E\mathrm{P}} d_{E\mathrm{P},0}\right)\right]. \tag{18}$$

Here, $\left|\rho_{\mathrm{D}M'}\right| << 1$ because the photoionization width $2\pi\left|d_{\mathrm{D},E\mathrm{P}}\right|^2 I$ is small as compared to the autoionization width Γ_{D}. Thus, one can neglect $t_{\mathrm{D}M'}$ in (15).

The second term of the right-hand side of (14) describes the interfering structure due to three resonances while the third term corresponds to the remaining five coupled resonances. Thus, the resulting structure contains contributions from eight resonances. However, only some of them can be observed in dependence on the polarization and propagation direction of the laser and probe radiation. Another restriction in the number of observed resonances is caused by the different dependencies of (11) and (12) on the field strength: at $F << 1$ the direct coupling is proportional to F while the coupling via the continuum is square dependent and is much weaker. In this case all the γ - couplings in (7) and (8) as well as the polarization shifts of the energies of the levels vanish. Moreover, the number of the direct P-D couplings can be reduced by special unitary transformations. For the subset (7), this transformation reads

$$\mathbf{U}_0 = \begin{bmatrix} \beta^* & 0 & \alpha^* \\ 0 & 1 & 0 \\ -\alpha & 0 & \beta \end{bmatrix}. \tag{19}$$

that leads to

$$\mathbf{H'_0} = \mathbf{U}_0\mathbf{H}_0\mathbf{U}_0^{+} = \begin{bmatrix} \mathcal{E}_D & -\frac{1}{2}\Omega_0 & 0 \\ -\frac{1}{2}\Omega_0 & \mathcal{E}_P & 0 \\ 0 & 0 & \mathcal{E}_D \end{bmatrix}. \tag{20}$$

where the D-states coupled to and decoupled from the $\mathrm{P}M = 0$ sublevel are defined by the superposition of the $\mathrm{D}M = \pm 1$ sublevels according to (19),

$$\left|\mathrm{D}_1^{(c)}\right\rangle = \beta^*\left|\mathrm{D}-1\right\rangle + \alpha^*\left|\mathrm{D}1\right\rangle,\ \left|\mathrm{D}_1^{(d)}\right\rangle = \beta\left|\mathrm{D}1\right\rangle - \alpha\left|\mathrm{D}-1\right\rangle. \tag{21}$$

respectively. Note that the continuum states of the decaying channels are transformed in the same manner. Thus the autoionizing widths of the transformed states do not change and they are not coupled via the decaying channels. The transformed Rabi frequency is

$$\Omega_0 = C_{10,11}^{21}\frac{d_{\mathrm{D,P}}F}{\sqrt{5}} = \frac{1}{\sqrt{10}}d_{\mathrm{D,P}}F\,. \tag{22}$$

An analogous transformation can be performed for $\mathbf{H}_1$ using

$$\mathbf{U}_1 = \begin{bmatrix} \frac{\sqrt{6}\beta AC}{\sqrt{N_2}} & 0 & \frac{\alpha^* A\left(C+2|\beta|^2\right)}{\sqrt{N_2}} & 0 & \frac{2\sqrt{6}\alpha^{*2}\beta A}{\sqrt{N_2}} \\ 0 & \frac{C}{\sqrt{N_1}} & 0 & \frac{2\alpha^*\beta}{\sqrt{N_1}} & 0 \\ -\frac{\alpha\beta^{*2}A\left(C+10|\alpha|^2+2\right)}{B\sqrt{N_2}} & 0 & -\frac{\sqrt{6}\beta^* A\left(C|\beta|^2-2|\alpha|^4\right)}{B\sqrt{N_2}} & 0 & \frac{\alpha^* A\left(A^2C+2|\alpha\beta|^2\right)}{B\sqrt{N_2}} \\ 0 & -\frac{2\alpha\beta^*}{\sqrt{N_1}} & 0 & \frac{C}{\sqrt{N_1}} & 0 \\ \frac{\alpha^2}{B} & 0 & -\frac{\sqrt{6}\alpha\beta}{B} & 0 & \frac{\beta^2}{B} \end{bmatrix}. \tag{23}$$

with $A = \sqrt{1+5|\beta|^2}$, $B = \sqrt{1+4|\alpha\beta|^2}$, $C = 5\left(|\alpha|^2 - |\beta|^2\right) + \sqrt{25-96|\alpha\beta|^2}$, $N_1 = C^2 + 4|\alpha\beta|^2$, and $N_2 = \left(A^2C + 2|\alpha\beta|^2\right)^2 + 24|\alpha\beta|^2$.

This gives

$$\mathbf{H'}_1 = \mathbf{U}_1\mathbf{H}_1\mathbf{U}_1^+ = \begin{bmatrix} \mathcal{E}_D & -\frac{1}{2}\Omega^{(1)} & 0 & 0 & 0 \\ -\frac{1}{2}\Omega^{(1)} & \mathcal{E}_P & 0 & 0 & 0 \\ 0 & 0 & \mathcal{E}_D & -\frac{1}{2}\Omega^{(2)} & 0 \\ 0 & 0 & -\frac{1}{2}\Omega^{(2)} & \mathcal{E}_P & 0 \\ 0 & 0 & 0 & 0 & \mathcal{E}_D \end{bmatrix}. \tag{24}$$

where

$$\Omega_1 = \frac{1}{A}\sqrt{\frac{N_2}{3N_1}}\Omega_0,\ \Omega_2 = AB\sqrt{\frac{2N_1}{N_2}}\Omega_0 \tag{25}$$

are the Rabi frequences for two couples of P and D states composed by their magnetic sublevels according to (23).

The transformation matrices (19) and (23) for the partial diagonalization (20) and (24) exist for arbitrary polarization and are independent of the laser field intensity. Using these results the cross section can be expressed in the more convenient form

$$\sigma(\Omega,F,\omega,\alpha,\varphi,b,\phi,\theta)=\sigma_d(\Omega)\left\{1-\sum_{j=0}^{2}\mathrm{Im}\left(\frac{A_j^{(+)}}{\Omega-\widetilde{\mathcal{E}}_j^{(+)}}+\frac{A_j^{(-)}}{\Omega-\widetilde{\mathcal{E}}_j^{(-)}}\right)\right\}. \qquad (26)$$

Here the complex energies and amplitudes of the resonances are

$$\widetilde{\mathcal{E}}_j^{(\pm)}=\frac{1}{2}\left(\mathcal{E}_{\mathrm{P}}+\mathcal{E}_{\mathrm{D}}\right)\pm\frac{1}{2}\sqrt{\left(\mathcal{E}_{\mathrm{P}}-\mathcal{E}_{\mathrm{D}}\right)^2+\Omega_j^2}\ . \qquad (27)$$

$$A_j^{(\pm)}=\pm\frac{1}{2}\Gamma_P\left|\widetilde{\varepsilon}_j\right|^2(q_P-i)^2\frac{\widetilde{\mathcal{E}}_j^{(\pm)}-\mathcal{E}_{\mathrm{D}}}{\widetilde{\mathcal{E}}_j^{(+)}-\widetilde{\mathcal{E}}_j^{(-)}}\ . \qquad (28)$$

with

$$\widetilde{\varepsilon}_0=\varepsilon^0\ ,\ \widetilde{\varepsilon}_1=\frac{C}{\sqrt{N_1}}\varepsilon^{-1}+\frac{2\alpha^*\beta}{\sqrt{N_1}}\varepsilon^1\ ,\ \widetilde{\varepsilon}_2=\frac{C}{\sqrt{N_1}}\varepsilon^1-\frac{2\alpha\beta^*}{\sqrt{N_1}}\varepsilon^{-1}\ . \qquad (29)$$

Thus, the $M=0$ pair of resonances does not depend on the laser polarization while the parameters of the other two pairs of resonances depend on the laser polarization through the Rabi frequences and the excitation strength. With decreasing laser intensity $\widetilde{\mathcal{E}}_j^{(+)}\to\mathcal{E}_{\mathrm{P}}$ and $\widetilde{\mathcal{E}}_j^{(-)}\to\mathcal{E}_{\mathrm{D}}$. This results in $A_j^{(-)}\to 0$ and $\sum_j A_j^{(+)}\to\frac{1}{2}\Gamma_{\mathrm{P}}(q_{\mathrm{P}}-i)^2$ and (26) transforms to the Fano formula for the isolate $2s2p\,^1P$ AIS.

The most important consequence that can be proven in studying the cross section, is that the resonances corresponding to the uncoupled (unperturbed) eigenvalues are invisible, because the corresponding states are composed from the DM sublevels for which $t_{DM}\approx 0$. Thus, no more than six resonances are observed, and the actual number depends on the polarization and relative propagation directions of the probe and dressed radiation. Note, that this is valid at laser intensities for which the induced width is much smaller than the autoionization one.

Results and discussion

Generally, the photoionization cross section depends on a set of parameters that characterize the probe and laser radiation. We study here the influence of the probe and laser polarization on the cross section under the condition of zero laser frequency detuning for coupling between the AISs.

Fig. 2 shows the photoionization cross section for different values of the laser intensity and for three values of the angle between the direction of the linear probe and the laser polarization. For an intensity $I < 5 \cdot 10^{-7}$ a.u. (Fig. 2a-c) the dependence on the polarization direction is weak. The difference increases however with increasing intensity. For collinear polarizations the results correspond to those obtained in [7]. The two resonances shown by solid curves in Fig. 2c correspond to the pair of coupled sublevels with M =0 with the quantization axis along the polarization direction. For perpendicular probe and pump polarizations (dotted curves) there are also two resonances, but they are shifted from those represented by the solid curve in Fig. 2d. This result can be explained by the fact that the coupling of the magnetic sublevels by the linearly polarized laser field depends only on the absolute value of M . In the case $\mathbf{F} \perp \mathbf{f}$ (dotted curve) the probe radiation can be represented by a superposition of two equal components with right-handed and left-handed circular polarization with respect to the laser polarization direction. Thus, the observed cross section corresponds to identical $M = \pm 1$ pairs of resonances. Moreover, for arbitrary polarized probe radiation propagating along the direction of the linear laser polarization, the same pairs of $|M| = 1$ resonances are observed. For an arbitrary angle between the linear polarization vectors, both pairs of resonances $|M|$ =0 and 1 contribute to the cross section as shown by the dashed curve in Fig. 2 for the angle 45^0 between **F** and **f** . Their relative intensities depend on the angle between the polarization vectors, while their separation increases with the laser intensity.

Fig. 3 presents the results at high laser intensity $I = 4 \cdot 10^{-6}$ a.u. for linear probe polarization and circular or elliptical laser polarization with different angles between the laser wave vector (quantization axis) and the probe polarization. The phase shift in (2) is $\varphi = -\pi / 2$. The ratio between the long and short ellipse axes is $\sqrt{3}$ and their orientation changes by 90^0 with respect to the plane of **f** and **k**. For the angle 0^0 between **f** and **k** (Fig. 3a) only the $M = 0$ pair is excited by the linear polarized probe radiation and the cross section is the same for arbitrary laser polarization, as established in the previous section. For the angles $\theta = 45^0$ and 90^0 between **f** and **k** (Fig. 3b,c) additional peaks appear in the cross section due to contributions from different $^1\mathrm{P}M$ sublevels coupled to the corresponding $^1\mathrm{D}M = \pm 1$ states by the elliptical laser field. The pair couplings differ according to the corresponding Rabi frequencies

(25). For the angle 45^0 (Fig. 3b) all three pairs of resonances with $M=-1,0,1$ are excited by the probe radiation. The $M=0$ pair of resonances has the same position as in Fig. 3a independently on the laser polarization, while the other resonances show shifts that depend on the polarization due to the Rabi frequencies (25). The relative resonance amplitudes depend on the ellipticity that defines the excitation strength of the corresponding transitions. For the angle 90^0 between **f** and **k** (Fig. 3c) the excitation of the $M=0$ state is forbidden.

Fig. 4 shows the results for the case of elliptically polarized probe and laser radiation (phase shifts: $\varphi=\phi=-\pi/2$, axes ratio: $\sqrt{3}$) with different axes alignments and angles between the wave vectors. In Fig. 4a ($\theta=0$) the ellipses coincide (solid curve) and are rotated by the angle 90^0 relatively to each other (dashed curve). In the last case, the relative strength of the $M=\pm1$ resonances is changed. When the probe wave vector rotates with respect to the long axis of the laser polarization ellipse, the $M=0$ sublevel contributes to the cross section. The strength of the $M=0$ resonances increases when θ changes from 45^0 (Fig. 4b) to 90^0 (Fig. 4c).

Fig. 5 shows the dependence of the cross section on the polarization helicity. The solid curves correspond to the case that the circularly polarized probe and laser radiation have the same helicity, while the results for opposite helicity of both radiations are shown by the dashed curves. The cross section at the angle $\theta=0$ and 45^0 (Fig. 5a and 5b, correspondingly) depends very sensitively on the helicity. For $\theta=90^0$, however, the result is the same for both, the right-handed and the left-handed polarization. The latter result follows from (5) and (29) according to which the sign of $\tilde{\varepsilon}_{\pm1}$ is different for opposite helicities so that the amplitudes (28) of the resonances are conserved.

At much higher laser intensities when the ionization width for the D state is essential and the pair resonance coupling breaks down, contributions from the other two D states should appear at the position near the unperturbed $2s2p\,^1P$ state. We do not consider this case here because, generally speaking, it is beyond the applicability of the rotation wave approximation.

Conclusions

In this paper, we considered the two autoionizing states $2s2p\,^1P$ and $2s3d\,^1D$ in helium which are resonantly coupled by an elliptically polarized laser field. We took into account all transitions between the magnetic sublevels which are induced by elliptically polarized laser radiation. For the photoionization cross section from the ground state which is caused by a probe radiation with arbitrary polarization, we obtained an analytical expression by using the non-Hermitian effective Hamiltonian method. In general, eight resonances contribute to the cross section. The results show that the resonant structure of the cross section in the vicinity of the $2s2p\,^1P$ state can considerably be modified by the polarization of the laser field. The cross section depends strongly also on the polarization and propagation direction of the probe radiation. At moderate laser intensities that are studied, there exist two states formed by the superposition of the ^1DM sublevels, which are not coupled to the ^1PM states and can thus not be observed in the cross section. For arbitrary laser polarization the other six resonances are coupled by pairs. Their relative strengths in the cross section vary with the laser and probe polarization. These results suggest an additional opportunity for the study of the atomic autoionization states by using lasers with different polarization.

Acknowledgments

We are indebted to A N Grum-Grzhimailo for valuable discussions. The work was supported, in part, by the Russian Foundation for Basic Research (project \# 04-02-17236).

The Bibliography

1. Karapanagioti, N.E., Charalambidis, D., Uiterwaal, C.J.G.J., et al., 1995, Phys. Rev. A, **53**, 2587.
2. Ganz, J., Raab, M., Hotop, H., and Geiger, J., 1984, Phys. Rev. Lett., **53**, 1547.
3. Lambropolous, P., and Zoller, P., 1981, Phys. Rev. A, **379**, 379.
4. Fedorov, M.V., and Kazakov, A.E., 1989, Progr. Quant. Electron., **13**, 1.
5. Bachau, H., Lambropoulos, P., and Shakeshaft, R., 1986, Phys. Rev. A, **34** 4785.
6. Kylstra, N.J., van der Hart, H.W., Burke, P.G., and Joachain, C.J., 1998, J. Phys. B: At. Mol. Opt. Phys., **31**, 3089.

7. Magunov, A.I., Rotter, I., and Strakhova, S.I., 1999, J. Phys. B: At. Mol. Opt. Phys., **32**, 1489.
8. Magunov, A.I., Rotter, I., and Strakhova, S.I., 1999, J. Phys. B: At. Mol. Opt. Phys., **32**, 1669.
9. Knight, P.L., Lauder, M. A., and Dalton, B., 1990, Phys. Rep., **190**,1.
10. Bohmer, K., Halfmann, T., Yatsenko, L.P., et al., 2002, Phys. Rev. A, **66**, 013406.
11. Kylstra, N.J., Paspalakis, E., and Knight, P.L., 1998, J. Phys. B: At. Mol. Opt. Phys., **31**, L719.
12. Magunov, A.I., Rotter, I., and Strakhova, S.I., 2001, J. Phys. B: At. Mol.Opt. Phys., **34**, 1489.
13. Heller, Yu.I., Lukinykh, V.F., Popov, A.K., and Slabko, V.V., 1981, Phys. Lett., **82A**, 4.
14. Eramo, R., Cavalieri, S., Fini, L., et al., 1997, J. Phys. B: At. Mol. Opt. Phys., **30**, 3789.
15. Liao, P.F., and Bjorklund, G.C., 1977, Phys. Rev. A, **15**,2009.
16. Georges, A.T., and Lambropoulos, P., 1978, Phys. Rev. A, **8**, 1072.
17. Chen, Y.-C., Lin, C.-W., and Yu, I.A., 2000, Phys. Rev. A, **61**, 053805.
18. McGloin, D., Dunn, M.H., and Fulton, D.J., 2000, Phys. Rev. A, **62**, 053802.
19. Moon, H.S., Kim, S.K., Kim, K., et al., 2003, J. Phys. B: At. Mol. Opt. Phys., **36**, 3721.
20. Milner, V., Chernobrod, B.M., and Prior, Y., 1999, Phys. Rev. A, **60**, 1293.
21. Morris, J.R., and Shore, B.W., 1983, Phys. Rev. A, **27**, 906.
22. Nienhuis, G., 1986, Opt. Commun., **59**, 353.
23. Smirnov, V.S., Tumaikin, A.M., and Yudin, V.I., 1989, Zhurn. Eksp. Teoret. Fiz., **96**, 1613.
24. Prudnikov, O.N., Tajchenachev, A.V., Tumaikin, A.M., Yudin, V.I., and Nienhuis, G. 2004, Zhurn. Eksp. Teoret. Fiz., **126**, 1613.
25. Fano, U., 1969, Phys. Rev., **178**, 131.
26. Sokell, E., Zamith, S., Bouchene, M.A., and Girard, B., 2000, Phys. B: At. Mol. Opt. Phys., **33**, 2005.
27. Nakajima, T., Nikolopoulos, L.A.A., 2003, Phys. Rev. A, **68**, 013413.
28. Pratt, S.T., Dehmer, P.M., and Dehmer, J.L., 1987, Phys. Rev. A, **35**, 3793.
29. Yi, J.-H., Lee, J., and Kong, H.J., 1995, Phys. Rev. A, **51**, 3053.

30. Rotter, I., 1991, Rep. Prog. Phys., **54**, 635.
31. Okolowicz, J., Ploszajczak, M., and Rotter, I., 2003, Phys. Rep., **374**, 271.
32. Gryslova, E.V., Magunov, A.I., Rotter, I., and Strakhova, S.I., 2005, Quantum Electron., **35**, 43.

Subscript.

1. Schematic presentation of the laser couplings between AISs in the He atom. Arrows indicate absorption (emission) of the right-handed circularly polarized photon (solid arrow) and absorption (emission) of the left-handed circularly polarized photon (dashed arrow). Dashed lines indicate continuum states.

2. Photoionization cross sections as a function of the reduced probe photon energy $\varepsilon = 2(\Omega - E_P)/\Gamma_P$ for linear probe and laser polarization and different values of the laser intensity: $I = 4\cdot 10^{-9}$ a.u. (a), $I = 4\cdot 10^{-8}$ a.u. (b), $I = 4\cdot 10^{-7}$ a.u. (c), and $I = 4\cdot 10^{-6}$ a.u. (d). The solid curves correspond to $\mathbf{F}\|\mathbf{f}$, the dashed curves are for the angle 45^0 between **F** and **f**, and the dotted curves are for $\mathbf{F}\perp\mathbf{f}$.

3. Photoionization cross sections for linear probe polarization parallel to the laser wave vector **k** (a), for the angle 45^0 between **f** and **k** (b), and for $\mathbf{k}\perp\mathbf{f}$ (c). The solid curves correspond to the circular laser polarization. The dashed curves are for the elliptical polarization with the long axis, **k** and **f** in the same plane. The dotted curves show the case when the short axis, **k** and **f** are in the same plane. The laser intensity is $I = 4\cdot 10^{-6}$ a.u..

4. Photoionization cross sections for elliptical polarization of the probe and laser radiation with collinear wave vectors $\mathbf{k}\|\mathbf{n}$ (a), for the angle 45^0 **k** and **n** (b), and for $\mathbf{k}\perp\mathbf{n}$ (c). The solid curves correspond to the case that the long axes of the probe and laser polarization ellipses coincide. The dashed curves show the case that the long axis of the laser polarization and the short axis of the probe polarization coincide. The laser intensity is $I = 4\cdot 10^{-6}$ a.u..

5. The same as in Fig. 4 but for circular polarization of the probe and laser radiation. The solid curves correspond to the same helicity of the probe and laser polarization and the dashed curves are for the case with opposite helicity of both radiations.}.

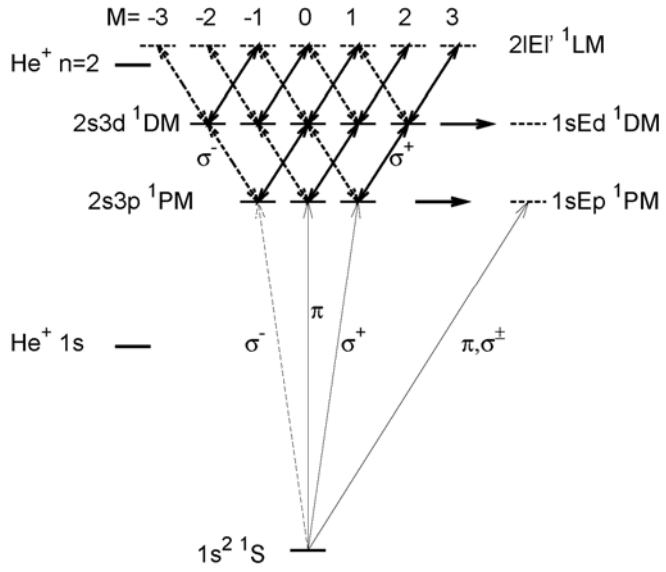
M= -3 -2 -1 0 1 2 3
He+ n=2
2s3d 1DM
2s3p 1PM
2lEl' 1LM
1sEd 1DM
1sEp 1PM
σ-
σ+
He+ 1s
π
σ-
σ+
π,σ±
1s2 1S

Fig. 1.

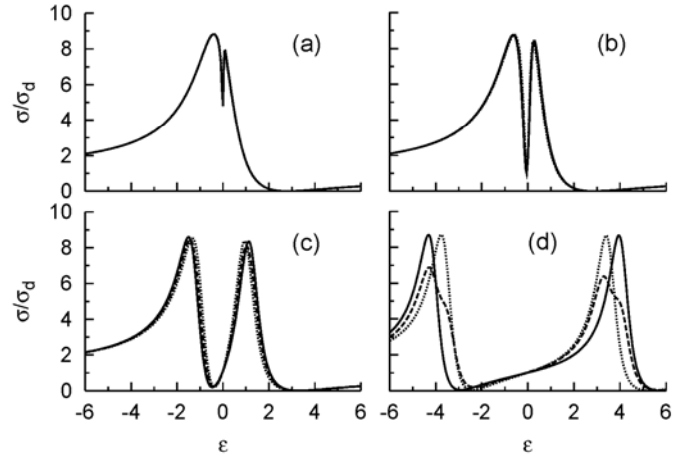

Fig. 2.

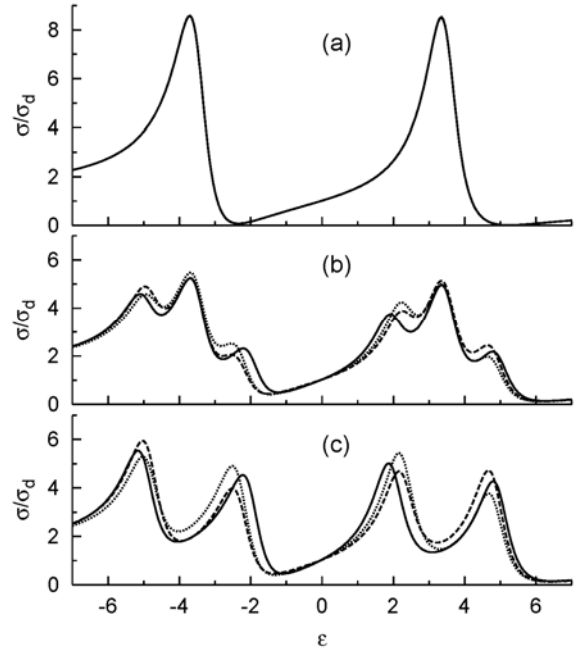

Fig. 3.

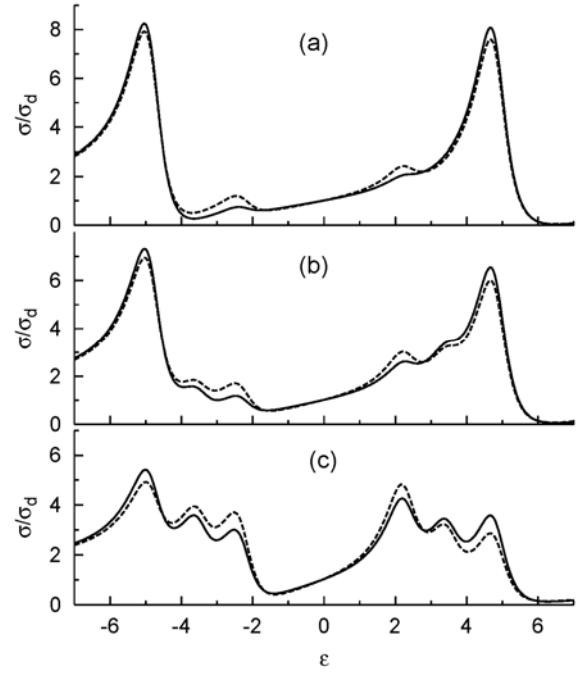

Fig. 4.

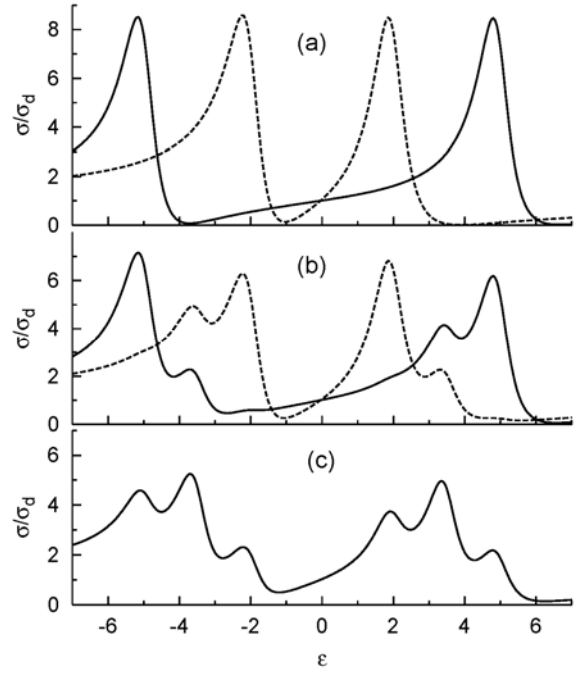

Fig. 5.

Elena Vladimirovna Gryzlova, Alexander Ivanovich Magunov, Ingrid Rotter, Svetlana Ivanovna Strakhova.

Laser polarization control of autoionization in helium atom.

Препринт НИИЯФ МГУ 2005-12/778

Работа поступила в ОНТИ 8.04.2005 г.

Издательство УНЦ ДО
ИД № 00545 от 06.12.1999

117246, Москва, ул.Обручева, 55-А, УНЦ ДО
т\ф (095) 718-65966, -7767, -7785 (комм.)
e-mail: abiturbook@mtu-net.ru
http://www.abiturbook.da.ru

Гигиенический сертификат № 77.99.2.925.П.9139.2.00 от 24.02.2000
Налоговые льготы – общероссийский классификатор продукции
ОК – 005 – 93, том 1 – 953000

Заказное. Подписано в печать _8.04.2005_г. Формат 60x90/16
Бумага офсетная №1. Усл.п.л. ___1,25____
Тираж …50….. экз. Заказ № ___793___

Отпечатано в Мини-типографии УНЦ ДО